[1.]L.O. JAYESIMI, [2.]M.A. WAHEED, [3.]M.G. SOBAMOWO

PREDICTION OF PEAK TEMPERATURES IN STRAIGHT AND TAPERED CYLINDRICAL TOOL PROFILES IN FRICTION STIR WELDING USING IMPROVED HEAT GENERATION MODELS

[1.] Works and Physical Planning Department, University of Lagos, Akoka, Lagos, NIGERIA
[2.] Department of Mechanical Engineering, Federal University of Agriculture, Abeokuta, NIGERIA
[3.] Department of Mechanical Engineering, University of Lagos, Akoka, Lagos, NIGERIA

Abstract: In this work, new model for the prediction of the peak temperatures in straight and tapered/conical cylindrical profiles FSW tools is presented through an improved analytical heat generation models. The developed models take into considerations that the welding process is a combination or mixture of the pure sliding and the pure sticking. From the obtained results, it is observed that increasing the tool rotational speed at constant weld speed increases the heat input, whereas the heat input decreases with an increase in the weld speed at constant tool rotational speed. Also, it was observed that the rate of heat generation at the shoulder is more in flat shoulder that the conical shoulder. The results in this work agreed with the experimental results. Therefore, the improved models could be used to estimate the heat generation in FSW tool.
Keywords: peak temperature; heat generation model; straight and tapered cylindrical tool profiles; friction stir welding

1. INTRODUCTION

The Friction stir welding (FSW), which is a contemporary relatively efficient novel solid-state welding method invented at The Welding Institute (TWI) of UK in 1991 has shown to be remarkably simple welding technique. It is considered to be the most significant development in metal joining in a decade and is a "green" technology due to its energy efficiency, environment friendliness, and versatility. However, in such significant welding technique, the fundamental knowledge of the thermal impact and thermo-mechanical processes of the technique is still not completely understood [1, 2]. Understanding the heat generation and the temperature history during the FSW process is the first step towards understanding the thermo-mechanical interaction taking place during the welding process. Modelling of heat generation and the optimum parameters during FSW can potentially accelerate the development of the welding process since the central issue in all cases is the determination of the heat input. In addressing the issue, several methods involving experimental analysis have been adopted to calibrate heat flow and maximum temperature but none of these approaches enable the heat generation and welding temperature to be predicted without an experimental measurement of some kind and in most cases, trial and error method is adopted. The determination of precise amount of heat generated during friction stir welding process is complicated since there are various uncertainties, assumptions and simplifications of mathematical model that describes welding process. Various experiments conducted around the planet, from the very beginning of the FSW method's application gave dispersive results about the generated heat. A more accurate and predictive approach uses the 3-dimensional flow field to calculate the heat generation from the material viscous dissipation. Even with these more sophisticated models there is conjecture over the best ways to describe the material behaviour, and the interface between the workpiece material and the tool, i.e. is there stick or slip. The analytical heat generation estimate correlates with the experimental heat generation, by assuming either a sliding or a sticking condition. However, the main uncertainties about process are when welding condition is a mixture of sliding and sticking. In this situation ambiguity of the value of the friction coefficient in every moment of the welding process, contact pressure between weld tool and weld pieces and shear stress are main reasons for difference between analytical and experimental result. The process of heat generation and peak temperature during FSW are complex and challenging tasks that require a multidisciplinary approach. Therefore, the seemingly simple task of predicting the weld heat generation and peak temperature has proved beyond the ability of most models. Previous works on modelling the FSW process for heat generation and peak temperature from the FSW tool are based on assumptions regarding the interface condition, which led some limitations and inaccuracies. In the model by Chao and Qi [3] developed heat generation model based on the assumption of sliding friction, where Coulomb's law is used to estimate the shear or friction force at the interface. Also, in their model, the pressure

at the tool interface is assumed to be constant, thereby enabling a radially dependent surface heat flux distribution as a representation of the friction heat generated by the tool shoulder, but neglecting that generated by the probe surface. Frigaardet al [4] modelled the heat input from the tool shoulder and probe as fluxes on squared surfaces at the top and sectional planes on a three-dimensional model and control the maximum allowed temperature by adjustment of the friction coefficient at elevated temperatures. Russell and Shercliff [5] based the heat generation on a constant friction stress at the interface, equal to the shear yield stress at elevated temperature, which is set to 5% of the yield stress at room temperature. Colegrove [6] uses an advanced analytical estimation of the heat generation for tools with a threaded probe to estimate the heat generation distribution. The fraction of heat generated by the probe is estimated to be as high as 20%, which leads to the conclusion that the analytical estimated probe heat generation contribution is not negligible. Also, the real situation during the welding process is a combination of the pure sliding and the pure sticking. Therefore, in this work improved analytical models are developed for the predictions of heat generation in straight and tapered/conical cylindrical profiles FSW tool. The developed models take into considerations that the welding process is a combination or mixture of the pure sliding and the pure sticking. The results in this work agreed with the conclusion of the past work. Therefore, the improved models could be used to estimate the heat generation in FSW tool.

It should be noted that the heat generation in FSW is a complex transformation process where one part of the mechanical energy is delivered to the workpiece, which is consumed in welding, while another is used for the deformation process and the rest of the energy is transformed into heat [7]. Ulysse [8] had earlier pointed out that 80-90% of the mechanical power delivered to the welding tool transforms into heat while recently, Pal and Phaniraj [9] showed that 10-20% of the total heat generated is transfer to the tool as shown in Table 1.

Table 1. Heat generation and heat partitioning with change in welding speed.

Welding speed, mm/s	Rotational speed, rpm	Friction heat (W)	Deformation heat (W)	Total heat generation (W)	Heat transfer to tool (W)	Heat partition (%)
60	560	1613	43	1656	343	79.24
80 (base case)	560	1625	56	1681	320	80.96
120	560	1731	84	1815	277	84.74

Source: Pal and Phaniraj [9]

In the process, heat is generated by friction (frictional heat) and by plastic deformation (plastic deformation). Both types of heat appear simultaneously on the FSW and they influence each other. Also, it should be noted that this heat is conducted to both the tool and the workpiece. The amount of the heat conducted into the workpiece dictates a successful FSW process, the quality of the weld, shape of the weld, micro-structure of the weld, as well as the residual stress and the distortion of the workpiece. The amount of the heat gone to the tool dictates the life of the tool and the capability of the tool for the joining process. Insufficient heat from the friction could lead to breakage of the pin of the tool since the material is not soft enough. Therefore, understanding the heat generation phenomena and the heat transfer aspects of the FSW process is fundamental to all other aspects of the welding process. Moreover, the influences of the tool geometry on thermal cycles, peak temperatures, power requirements, and torque during FSW processes are complex and remain to be fully understood. Consequently, the tool design is currently carried out by trial and error methods. The current effort in this work is directed towards development of mathematical models that will predict the maximum temperature during frictional stir welding.

2. DEVELOPMENT OF HEAT GENERATION MODELS FOR THE FRICTION STIR WELDING

Consider the friction stir welding (FSW) shown schematically in Figure 2. During the FSW, a rotating tool moves along the joint interface. As the tool moves along the joint and into the workpiece, heat generated at surface and near the interface between the tool and the work-piece is transported into the workpiece and the tool (Figure 2). The total heat generated at different portions of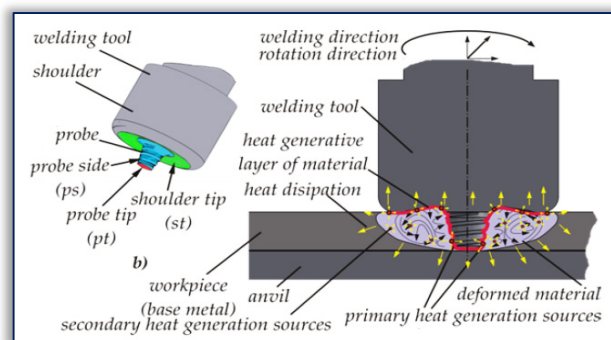 the tool is the summation of the heat generated at the tool shoulder surface, heat generated at the tool pin/probe side and the heat generated at the tool pin/probe tip.

Figure 2. Heat generation in FSW (Mijajlović and Milčić) [11]

Also, during the frictional stir welding, heat is generated by pure sliding (adhesion) and pure sticking (deformation). In pure sliding condition, it is assumed that there is shear in the contact interface and can be

described as fully Coulomb friction condition. In the assumption, the contact pressure between tool and weld piece p and friction coefficient μ are constant or linearly dependable values from various variables. The shear stress becomes equals to dynamic contact shear stress. In the pure sticking, it is assumed shearing in the layer of the material of weld pieces very close to the contact surface and uniformity of the shear stress τ. In this situation, surface of the weld piece will stick to the moving tool's surface only if friction shear stress exceeds the yield shear stress of the weld piece. The real situation during welding process gives combination of the pure sliding and the pure sticking. Therefore, it is absolutely correct to say that heat generating during friction stir welding is product of pure sliding, pure sticking and combination of sliding and sticking [10].

⊞ Model development for heat generation for flat circular/straight cylindrical tool

As pointed out, in this work, the heat generated in FSW was considered to be due to friction (due total sliding condition only), but practically, it is due to friction as well as deformation (due to sticking condition) [7]. Considering both types of heat and their influence on each other, the total amount of heat generated on the pin tip, pin side and the shoulder tip are respectively given by

$$Q_{pt} = (1-\delta_{pt})Q_{pt}^{fr} + \delta_{pt}Q_{pt}^{def} \qquad (1)$$

$$Q_{ps} = (1-\delta_{ps})Q_{ps}^{fr} + \delta_{ps}Q_{ps}^{def} \qquad (2)$$

$$Q_{st} = (1-\delta_{st})Q_{st}^{fr} + \delta_{st}Q_{st}^{def} \qquad (3)$$

where the heat indexed with fr represents frictional heat, heat indexed with def represents deformation heat, δ_{pt}, δ_{ps}, δ_{st} are dimensionless contact state variable (extension of slip) at the pin tip, pin side and shoulder tip, respectively. It should be noted that δ_{pt}=0.1, δ_{ps}= 0.2 and δ_{st}= 0.1 [12]. It should be noted that If δ is 1, full sticking condition is applied and all the heat is generated by plastics deformation. When $\delta = 0$, heat is generated only by friction.

The analytical estimation based on a general assumption of uniform contact shear stress $\tau_{contact}$ is considered.

— Weld cycle excludes plunging; first, second dwell, and retract cycles.

— Tool inclination angle was not considered.

— No heat flows into the workpiece if the local temperature reaches the material melting temperature.

— The axial pressure is evenly distributed along z-axis

— Due to friction and deformation interface conditions, the frictional and deformation shear stresses are considered.

— The thread on the pin side of the welding tool was neglected
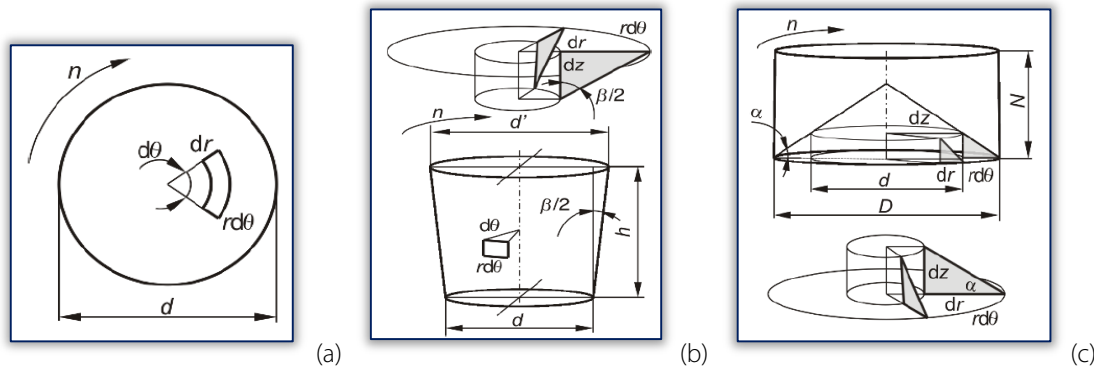

(a)   (b)   (c)

Figure 3. Active surfaces in FSW: (a) pin tip, (b) pin side, (c) shoulder tip

The general expression for an infinitesimal amount of heat generation at each of the different zones of the tool / workpiece interface is given by

$$dQ = \omega r dF \qquad (4)$$

where dQ is the heat generated per unit time, dF is the force acting on the surface at a distance r from the tool centerline and ω is the angular velocity of the tool.

$$dF = \tau_{contact} dA \qquad (5)$$

where $\tau_{contact}$ is the contact shear stress and $dA = rdrd\theta$ is the area of the infinitesimal segment on the surface. The frictional and deformation amount of heat with respect to the contact shear stress is given by:

$$\tau_{cont} = \begin{cases} \mu p & \text{for frictional heat generation (Coulomb's friction law)} \\ \tau_{yield} & \text{for deformational heat generation} \end{cases} \qquad (6)$$

where μ is the frictional coefficients, p is the contact pressure, τ_{yield} is the yield strength of the workpiece.

Following Arora et al. [13, 14], frictional coefficients can be calculated as:

$$\mu = \mu_o exp\left(-\delta_{slip}\frac{\omega}{\omega_o}\frac{R_p}{R_s}\right) \tag{7}$$

where μ_o is the static friction coefficient and it is taken as 0.45 [15, 16]. δ_{slip} is the slipping factor, ω is the rotating speed and the reference rotation speed ω_o is taken as 400 rpm. R_p and R_s are the radii of the tool pin and the shoulder, respectively.

Substituting Eqs. (5) and (6) into Eq. (4) and integrate, for the shoulder tip frictional heat generation, gives:

$$Q_{st}^{fr} = \int_0^{2\pi}\int_{R_p}^{R_s} u\mu p r dr d\theta \tag{8}$$

$$Q_{st}^{fr} = \int_0^{2\pi}\int_{R_p}^{R_s} \mu p(\omega r \pm v_w sin\theta) r\ dr d\theta \tag{9}$$

where $u = \omega r \pm v_w Sin\theta$, the positive and the negative sign denote advancing and retracting movement of the tool. v_w is the welding velocity:

$$Q_{st}^{fr} = \mu p \int_0^{2\pi}\int_{R_p}^{R_s}(\omega r^2 \pm r v_w sin\theta) dr d\theta \tag{10}$$

$$Q_{st}^{fr} = \mu p\left[\int_0^{2\pi}\int_{R_p}^{R_s}\omega r^2 dr d\theta \pm \int_0^{2\pi}\int_{R_p}^{R_s} r v_w sin\theta dr d\theta\right] \tag{11}$$

After the integration, one arrives at:

$$Q_{st}^{fr} = \frac{2}{3}\pi\omega\mu p\left(R_s^3 - R_p^3\right) \tag{12}$$

Similarly, for the shoulder tip deformational heat generation,

$$Q_{st}^{def} = \frac{2}{3}\pi\omega\tau_{yield}\left(R_s^3 - R_p^3\right) \tag{13}$$

The total heat generation at the shoulder tip is:

$$Q_{st} = \frac{2}{3}\pi\omega\mu p\left(R_s^3 - R_p^3\right)(1-\delta_{st}) + \frac{2}{3}\pi\omega\tau_{yield}\delta_{st}\left(R_s^3 - R_p^3\right) \tag{14}$$

It should be noted that not all the mechanical energy is converted to frictional and deformational heat.

$$Q_{st\eta} = \frac{2}{3}\pi\omega\eta_{fd}\left[\mu p\left(R_s^3 - R_p^3\right)(1-\delta_{st}) + \tau_{yield}\delta_{st}\left(R_s^3 - R_p^3\right)\right] \tag{15}$$

The total heat generation at the interfaces is the summation of the total heat generation at the shoulder tip, total heat generation at the pin tip and total heat generation at the pin side i.e.

$$Q_{total} = Q_{st\eta} + Q_{pt\eta} + Q_{ps\eta} \tag{16}$$

For the flat shoulder and flat pin, total heat generation at the interfaces is given as:

$$Q_{total} = \frac{2}{3}\pi\omega\eta_{fd}\left[\begin{array}{l}\mu p\left(R_s^3 - R_p^3\right)(1-\delta_{st}) + \tau_{yield}\delta_{st}\left(R_s^3 - R_p^3\right) + \mu p R_p^3(1-\delta_{pt}) \\ +\tau_{yield}\delta_{pt}R_p^3 + \mu p R_p^2 L_p(1-\delta_{ps}) + \tau_{yield}R_p^2 L_p\delta_{ps}\end{array}\right] \tag{17}$$

The energy per unit length of the weld of the flat shoulder and flat pin tool is

$$Q'_{Enery} = \frac{2\pi\omega\eta_{fd}}{3vR_s^2}\left[\begin{array}{l}\mu p\left(R_s^3 - R_p^3\right)(1-\delta_{st}) + \tau_{yield}\delta_{st}\left(R_s^3 - R_p^3\right) + \mu p R_p^3(1-\delta_{pt}) \\ +\tau_{yield}\delta_{pt}R_p^3 + \mu p R_p^2 L_p(1-\delta_{ps}) + \tau_{yield}R_p^2 L_p\delta_{ps}\end{array}\right] \tag{18}$$

⊞ Model development for heat generation for conical circular / straight cylindrical tool

Also, the heat generation models for conical/tapered tool are derived in similar way as shown above in Eq. (4), (5) and (8-18).

For the conical shoulder and flat pin, total heat generation at the interfaces is given as:

$$Q_{total} = \frac{2}{3}\pi\omega\eta_{fd}\left[\begin{array}{l}\mu p\left(R_s^3 - R_p^3\right)(1-\delta_{st})(1+tan\alpha) + \tau_{yield}\delta_{st}\left(R_s^3 - R_p^3\right)(1+tan\alpha) \\ +\mu p R_p^3(1-\delta_{pt}) + \tau_{yield}\delta_{pt}R_p^3 + \mu p R_p^2 L_p(1-\delta_{ps}) + \tau_{yield}R_p^2 L_p\delta_{ps}\end{array}\right] \tag{19}$$

If the shoulder is flat and the pin conical, total heat generation at the interfaces:

$$Q_{total} = \frac{2}{3}\pi\omega\eta_{fd}\left[\begin{array}{l}\mu p\left(R_s^3 - R_p^3\right)(1-\delta_{st}) + \tau_{yield}\delta_{st}\left(R_s^3 - R_p^3\right) + \mu p R_p^3(1-\delta_{pt}) + \tau_{yield}\delta_{pt}R_p^3 \\ +\mu p R_p^2 L_p\left(1+tan\frac{\beta}{2}\right)(1-\delta_{ps}) + \tau_{yield}R_p^2 L_p\delta_{ps}\left(1+tan\frac{\beta}{2}\right)\end{array}\right] \tag{20}$$

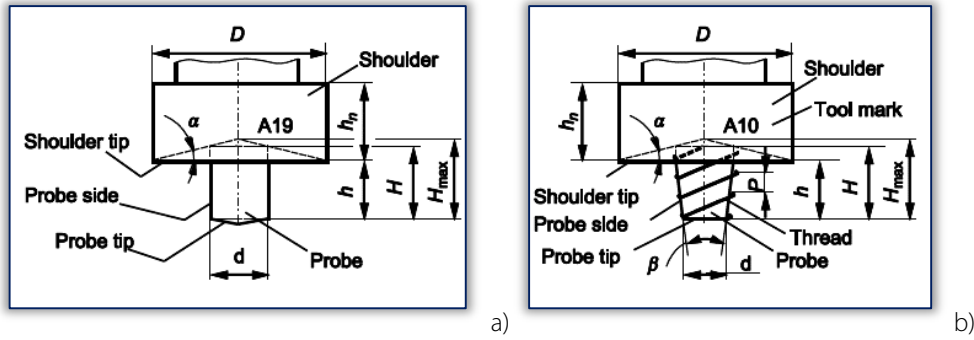a)   b)

Figure 4. FSW tool (a) conical shoulder with flat pin (b) conical shoulder with conical pin, D=R_p and d= R_s[26]

The energy per unit length of the weld of the flat shoulder conical pin tool is:

$$Q'_{Energy} = \frac{2}{3}\frac{\pi\omega\eta_{fd}}{vR_s^2}\left[\begin{array}{c}\mu p\left(R_s^3 - R_p^3\right)(1-\delta_{st}) + \tau_{yield}\delta_{st}\left(R_s^3 - R_p^3\right) + \mu pR_p^3(1-\delta_{pt}) + \tau_{yield}\delta_{pt}R_p^3 \\ +\mu pR_p^2 L_p\left(1+tan\frac{\beta}{2}\right)(1-\delta_{ps}) + \tau_{yield}R_p^2 L_p\delta_{ps}\left(1+tan\frac{\beta}{2}\right)\end{array}\right] \tag{21}$$

If the shoulder and the pin are conical with different conical angles, total heat generation at the interfaces:

$$Q'_{Energy} = \frac{2}{3}\pi\omega\eta_{fd}\left[\begin{array}{c}\mu p\left(R_s^3 - R_p^3\right)(1-\delta_{st})(1+tan\alpha) + \tau_{yield}\delta_{st}\left(R_s^3 - R_p^3\right)(1+tan\alpha) + \mu pR_p^3(1-\delta_{pt}) \\ +\tau_{yield}\delta_{pt}R_p^3 + \mu pR_p^2 L_p\left(1+tan\frac{\beta}{2}\right)(1-\delta_{ps}) + \tau_{yield}R_p^2 L_p\delta_{ps}\left(1+tan\frac{\beta}{2}\right)\end{array}\right] \tag{22}$$

The energy per unit length of the weld for the conical shoulder tool is:

$$Q'_{Energy} = \frac{2}{3}\frac{\pi\omega\eta_{fd}}{vR_s^2}\left[\begin{array}{c}\mu p\left(R_s^3 - R_p^3\right)(1-\delta_{st})(1+tan\alpha) + \tau_{yield}\delta_{st}\left(R_s^3 - R_p^3\right)(1+tan\alpha) + \mu pR_p^3(1-\delta_{pt}) \\ +\tau_{yield}\delta_{pt}R_p^3 + \mu pR_p^2 L_p\left(1+tan\frac{\beta}{2}\right)(1-\delta_{ps}) + \tau_{yield}R_p^2 L_p\delta_{ps}\left(1+tan\frac{\beta}{2}\right)\end{array}\right] \tag{23}$$

where η_{fd} represents the fraction of the mechanical energy that is converted to frictional heat and deformational heat. Which could be as high as 0.99 based on the assumptions of previous work.

The boundary value of the yield shear stress from the von Misses yield criterion in uniaxial tension and pure shear is given by:

$$\tau_{yield} = \frac{\sigma_{yield}(T,\varepsilon)}{\sqrt{3}} \tag{24}$$

The yield strength of the workpiece's material $\sigma_{yield}(T,\varepsilon)$ is highly dependent on temperature, T and strain rate, ε. The analysis of the tangential stresses within FSW requires the full temperature and strain history in the workpiece in a wide zone around the welding tool. Sheppard and Wright [17] elastic-plastic model may be used to evaluate the temperature-strain dependent yield strength of the workpiece's material, $\sigma_{yield}(T,\varepsilon)$.

$$\sigma_{yield}(T,\varepsilon) = \frac{1}{\alpha}sinh^{-1}\left[\left(\frac{Z(\varepsilon,T)}{A}\right)^{\frac{1}{n}}\right] \tag{25}$$

where A, α, and n are material constants and Z(ε,T) is the Zener-Hollomon parameter that represents the temperature-compensated effective strain rate by:

$$Z(\varepsilon,T) = \dot{\varepsilon}e\,xp\left(\frac{Q}{RT}\right) \tag{26}$$

where $\dot{\varepsilon}, Q, R, and\ T$ are strain rate, activation energy, universal gas constant and absolute temperature, respectively.

Sheppard and Jackson [18] developed the elastic-plastic model for yield strength of the workpiece's material as:

$$\sigma_{yield}(T,\varepsilon) \approx \frac{1}{\alpha}In\left\{\left(\frac{Z(T,\varepsilon)}{A}\right)^{\frac{1}{n}} + \left[1+\left(\frac{Z(T,\varepsilon)}{A}\right)^{\frac{2}{n}}\right]^{\frac{1}{2}}\right\} \tag{27}$$

It was stated that the lack of the detailed material constitutive information and other thermal and physical properties at conditions such as very high strain rates and elevated temperatures seems to be the limiting factor

while modeling the FSW process [19]. Consequently, Colegrove and Sherchiff [20] and Wang et al., [21] pointed out that Sheppard and Jackson's elastic-plastic model is not applicable at the melting of the material. Although, Su et al. [22] modified the Sheppard and Jackson's elastic-plastic model as:

$$\sigma_{yield}(T,\varepsilon) = \sigma_o + \left\{ \frac{1}{\alpha} \left(1 - \sqrt{\frac{T-273}{T-273}} \right) In \left\{ \left(\frac{Z(T,\varepsilon)}{A} \right)^{\frac{1}{n}} + \left[1 + \left(\frac{Z(T,\varepsilon)}{A} \right)^{\frac{2}{n}} \right]^{\frac{1}{2}} \right\} \right\} \tag{28}$$

However, analysis of heat generation in FSW can neglect the influence of strain on the decrease of yield strength and still maintain sufficient precision [23]. Neglecting strain effects on the yield strength is possible since the maximal temperatures of the material reach about 80% of the melting temperature when the strain has significant values due to near melting conditions in the material [13 and 14]. Therefore, Eq. (16) becomes:

$$\tau_{yield} = \frac{\sigma_{yield}(T)}{\sqrt{3}} \tag{29}$$

For Stainless steel, yield stress as developed in this work:

$$\sigma_{yield}(T) = \beta_o + \beta_1 T + \beta_2 T^2 + \beta_3 T^3 + + \beta_4 T^4 + + \beta_5 T^5 \tag{30}$$

where: $\beta_o = 240$, $\beta_1 = 7.3583 \times 10^{-1}$, $\beta_2 = -7.1333 \times 10^{-2}$, $\beta_3 = 2.163 \times 10^{-5}$,

$\beta_4 = -2.7292 \times 10^{-8}$ and $\beta_5 = 1.1849 \times 10^{-8}$

3. MODELING THE PEAK TEMPERATURE IN FRICTION STIR WELDING

The published works in literature point to the fact that there is an optimum temperature range to obtain defect-free joints and such a range has not been specified. However, a number of researchers as shown that there is a linear regression of the temperature ratio T_{peak}/T_s (where Tpeak is the peak/maximum temperature and Ts is the solidus temperature) on T_s was derived: where this temperature range can be thought of as the optimum temperature range, i.e. $T_{peak} = T_{opt}$. The correlation has a standard deviation of 0.024. The calculation results in a temperature range $T_{opt} = (0.8–0.9) T_s$. The rationality of this assumption was verified by experiments [24]. The linear relationship is given by

$$\frac{T_{peak}}{T_s} = \frac{T_{opt}}{T_s} = \psi_1 + \psi_2 T_s \tag{31}$$

which gives

$$T_{peak} = (\psi_1 + \psi_2 T_s) T_s \tag{32}$$

where ψ_1 and ψ_2 are to be determined from experiment e.g. for Aluminum alloy 1100-H14 and 2024-T3 rolled plates 8 and 3.2 mm in thick, $\psi_1 = 1.344$ and $\psi_2 = 0.0005917$.

Also, empirical model developed by Hamilton et al. [25] shown in Eq. (74) could be adopted:

$$\frac{T_{peak}}{T_s} = 0.54 + 0.000156 Q_{max} \tag{33}$$

where

$$Q_{max} = \varphi Q'_{Energy} \tag{34}$$

φ is the ratio of the pin length L_p to the workpiece thickness, t. Q'_{Energy} are defined in Eq. (17), (18), (21) and (22) for straight and tapered tools. In this work, our analysis establishes a non-linear regression of the peak temperature and maximum heat generation, Q_{max}

$$T_{peak} = \xi (Q_{max} \overline{Q})^\gamma \tag{35}$$

Also, $\overline{Q}$ is the non-dimensional heat input, which is defined as [26]:

$$\overline{Q} = \frac{\sigma_8 S \omega C \eta}{k_w v^2} \tag{36}$$

where, for conformity of calculation, the unit of ω changes from rpm to rad m/s and v from mm/min to m/s, σ_8 is the yield stress of the material at a temperature of 0.8Ts, S is the cross-sectional area of the tool shoulder, C is the specific heat capacity of the workpiece material, k_w is the thermal conductivity of the workpiece, and η is the ratio according to which heat generated at the shoulder–workpiece interface is transported between the tool and the workpiece, and is defined as

$$\eta = \frac{\sqrt{(k\rho c_p)_w}}{\sqrt{(k\rho c_p)_T}} \qquad (37)$$

and

$$v = \frac{\pi N r}{30 n \alpha \sigma_{yield}(T, \varepsilon)} \qquad (38)$$

Substituting Eq. (38) into Eq. (36), one arrives at:

$$\overline{Q} = \frac{\sigma_s S\left(\dfrac{\pi N}{30}\right) C \eta}{k_w \left\{ \dfrac{\pi N r}{30 n \alpha \sigma_{yield}(T, \varepsilon)} \right\}^2} \qquad (39)$$

Also, substituting Eq. (39) into Eq. (35), gives:

$$T_{peak} = \xi \left\{ Q_{max} \frac{\sigma_s S\left(\dfrac{\pi N}{30}\right) C \eta}{k_w \left\{ \dfrac{\pi N r}{30 n \alpha \sigma_{yield}(T, \varepsilon)} \right\}^2} \right\}^{\gamma} \qquad (40)$$

4. RESULTS AND DISCUSSIONS

Figure 5 shows the influence of shoulder radius on the rate of heat generation at the shoulder-workpiece, Aluminum alloys (AA-6061-T6).
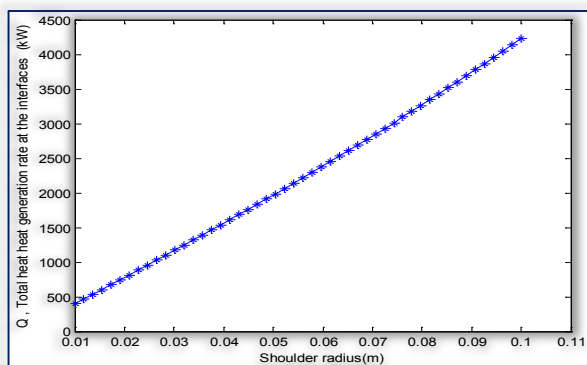
Figure 5. Variations total heat generation rate at the interfaces with shoulder radius
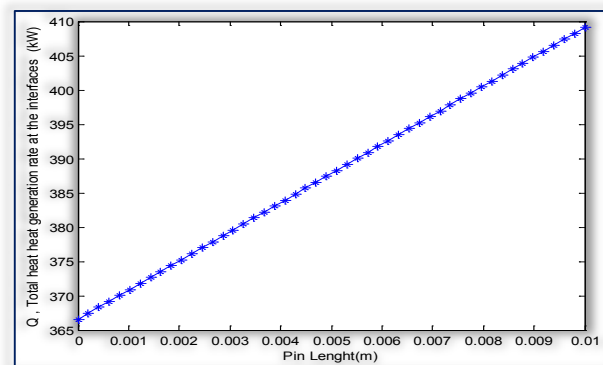
Figure 6. Variations total heat generation rate at the interfaces with pin length

It could be inferred from the results that the shoulder radius is directly proportional to the total heat generated rate at the interface. i.e. as the shoulder radius increases, the rate at which heat is generated at the interface increases. The same trend was noticed in Figure 6 and 7 where the total heat generation rate increases with increase in pin length and pin radius. This heat propagates either through conduction in the various parts of the workpiece and the tool or through convection to the environment. In addition, higher heat generation due to plastic deformation and smaller interfacial contact area with the workpiece leads to lower frictional heat generation relative to the pin. The failure of friction stir welded joints takes place at the heat-affected zone (HAZ) where the density of the needle-shaped precipitate is less. From the fractional heat generation rate analysis carried out in this study, it is shown that depending on the welding conditions, between 80 to 90% heat is generated at the tool shoulder and the remaining amount at other tool surfaces. This fact has also been confirmed in the experimental work carried out by Nandan et al. [28]. Indisputably, the proportion of the heat generated at the tool shoulder and the pin surfaces is determined by the tool geometry and the welding variables [28]. Also, from the reported literature, it is understood that the pin geometry plays a vital role for material flow, temperature history, grain size, and mechanical properties in the FSW process [7]. Figure 8 and 9 effects of angle of rotation on rate of heat generation when the extent of sticking are 0.65 (sticking and sliding condition) and 1 (full sticking condition). The non-uniformity in the heat generation pattern results from the difference in the relative velocity at different angular locations on the pin surface, which arises due to the variation in term $U sin\theta$.

The angular variations of temperature on the tool surface results from the local differences in the heat generation rates. Therefore, meaningful modeling of temperature and plastic flow fields must consider 3D heat

transfer [29]. Figure 10 shows the variations of heat generation with angle of rotation when the extent of sticking is 0 (full sliding condition). The result depicts that angle of rotation has no effect on the rate of heat generation when the extent of sticking is 0 as a constant value line is shown in the figure.
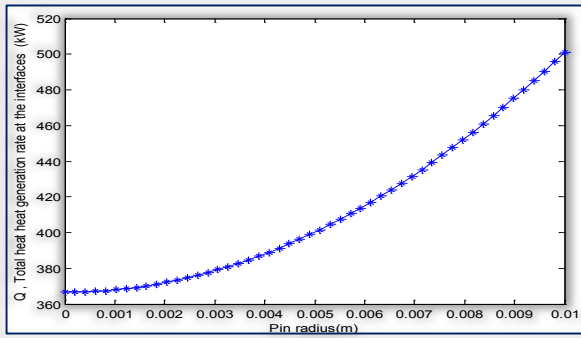

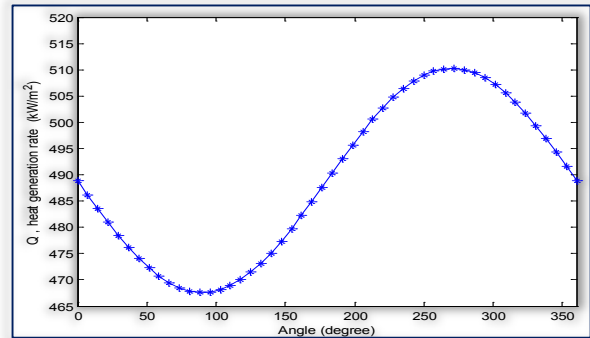Figure 7. Variations total heat generation rate at the interfaces with pin radius

Figure 8. Variations heat generate with angle of rotation when the extent of sticking is 0.65
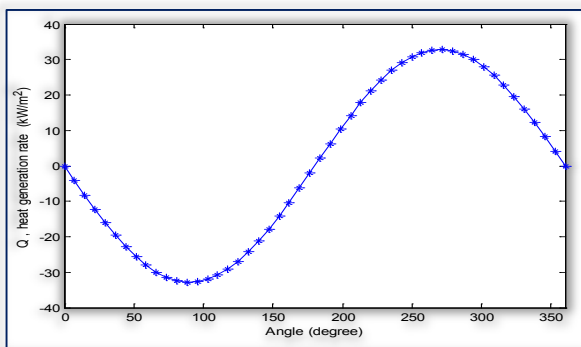

Figure 9. Variations heat generate with angle of rotation when the extent of sticking is 1 (full sticking condition)
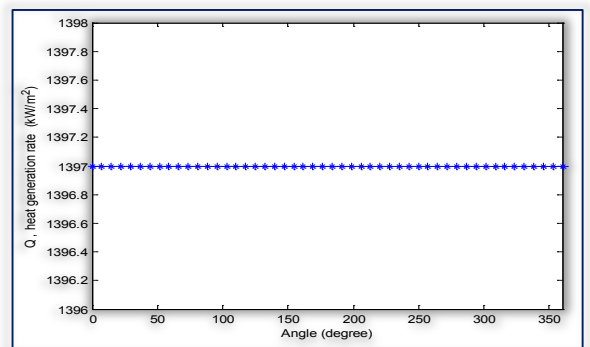

Figure 10. Variations heat generate with angle of rotation when the extent of sticking is 0 (full sliding condition)
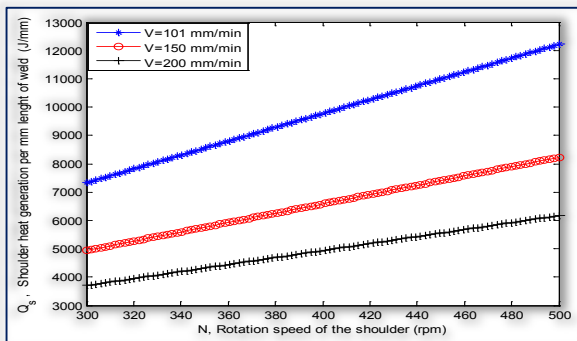

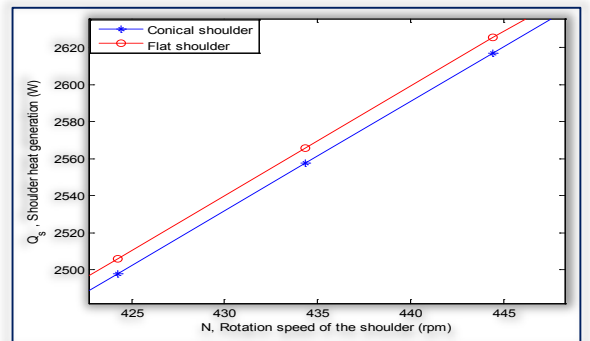Figure 11. Effects of welding speed on the heat generation at the shoulder

Figure 12. Effects of shoulder conical angle on the heat generation at the shoulder

Figures 11-13 present the effects of shoulder rotation speed, conical angle and contact conditions on heat generation. Figure 11 shows variation of shoulder heat generation rate with welding rotational speed at different welding velocities of 101, 150 and 200 mm/min. while Figure 12 shows the variation of shoulder heat generation with rotational speed of the shoulder at for conical and flat shoulders. As it could be seen from Figure 11, that the rate of heat generated at the shoulder varies inversely proportional with the welding speed. This is due to the fact that at higher welding velocity, the heat input per unit length decreases as heat is dissipated over a wider region of the workpiece. At high rotational speed, the relative velocity between the tool and workpiece is high, and consequently the heat generation rate and the temperatures are also high. The rate of heat generation at the shoulder is more in flat shoulder that the conical shoulder as shown in Figure 12. This is because the flatness of the shoulder tip increases the tool-workpiece contact surfaces and thereby creating more friction during the process to generate frictional heat and consequently, increases the rate of heat generation. This inference is clearly depicted in Figure 12. The influence of contact condition variables on the rate of heat generation at the shoulder and the pin as displayed in Figure 13. As expected, the heat

generation rate increases with the increase in contact condition variables because more heat are generated due to friction due to increased contacts between the tool and the workpiece.

For the experimental conditions studied by Nandan et al. [27], the computed heat generation rates at the shoulder and the pin surfaces are presented in Table 2. The results show that depending on the welding conditions, between 80 to 90% heat is generated at the tool shoulder and the remaining amount at other tool surfaces. As shown in the results, the heat inputs from the shoulder and the pin as well as the maximum temperature of the workpiece increase with the weld and rotational speeds.
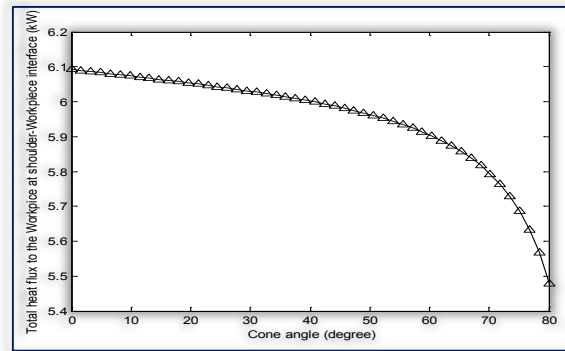

Figure 13. Effects of conical angle on the heat generation at the shoulder-workpiece interface
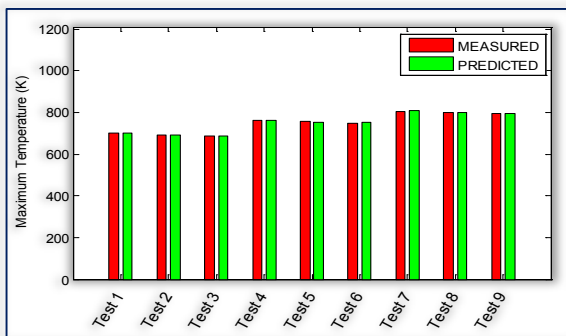

Figure 14. Bar chart for comparison of results for maximum temperature in Aluminum alloy
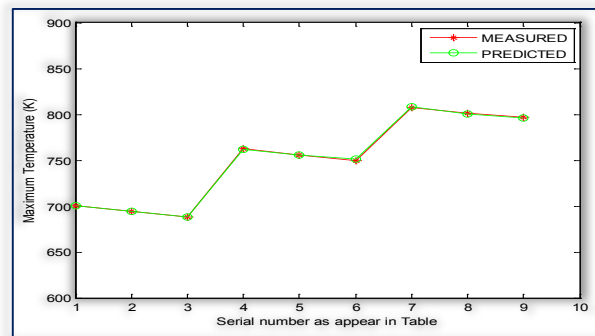

Figure 15. Line graph for comparison of results for maximum temperature in Aluminum alloy

Table 2. Variation of heat generated and peak temperature at the tool shoulder and the pin surfaces welding variables

S/N	Weld Speed (mm/s)	Rotational Speed (rpm)	Heat Input from Shoulder (KW)	Heat Input from Tool Pin (W)	Heat Input from Tool Bottom (W)	Maximum Temperature (K) (measured)	Maximum Temperature (K) (Predicted)
1	0.5	200	2.97	250.1	45.6	700.2	700.311
2	1	200	3.05	252.8	46.1	694.4	694.434
3	1.5	200	3.17	258.5	47.7	688.2	687.914
4	0.5	400	3.72	213.9	61.9	762.7	761.789
5	1	400	3.72	215.5	62.1	756	755.573
6	1.5	400	3.88	216.2	63.4	749.6	751.346
7	0.5	600	4.23	164.3	76.2	807.4	808.654
8	1	600	4.31	168.1	77	801.5	800.795
9	1.5	600	4.47	172.3	77.4	797.3	796.480

From the analysis, it was found that the average absolute error between the experimental and the predicted maximum temperature is 0.090799, while average bias error of correlation is 0.00006446, the normalized standard deviation is 0.12047, correlation coefficient is 0.99961 and the Coefficient of multiple determination is 0.99953. Good agreements between the experimentally determined and the computed results at different monitoring locations indicate that the model can be used to examine the temperature profiles and cooling rates.

5. CONCLUSION

In this work, new model for the prediction of the peak temperatures in straight and tapered/conical cylindrical profiles FSW tools has been developed through an improved analytical heat generation models. The developed models take into considerations that the welding process is a combination or mixture of the pure sliding and the pure sticking. The results agreed with experimental results. Therefore, the improved models could be used to estimate the heat generation in FSW tool.

Nomenclature
A area, m^2
F axial force/N
f_s shoulder heat generation ratio from shoulder

Q heat generation, W
Qs heat generation from the shoulder side, W
Qp heat generation from the probe side, W

Q_{Total} total heat generation/W
τ friction shear stress, Pa
p contact pressure, Pa
σ contact pressure, Pa
μ friction coefficient

v tool tool speed of ωr, ms−1
δslip slip rate at interface, ms−1
θ angle, deg
z dimension along rotation axis, m
α tool shoulder cone angle, deg

f_{ps} probe side heat generation ratio from probe side
f_{pt} probe tip heat generation ratio from probe tip
HProbe tool probe height/mm
H_p tool probe height, m

Q_t heat generation from the tip, W
R shoulder tool shoulder radius, m
R_p tool probe radius, m

ω tool angular rotation speed, rad s−1
δ contact state variable
r position along tool radius, m

τ_y yield shear stress, Pa
σ_y yield yield stress, Pa

References

[1]   W. M. Thomas, E. D. Nicholas, J. C. Needham, M. G. Murch, P. Temple-Smith and C. J. Dawes, Friction-Stir Butt Welding, GB Patent No. 9125978.8, International Patent Application No. PCT/ GB92/02203, 1991.

[2]   J. A. Schneider. Temperature Distribution and Resulting Metal Flow. In: Mishra RS, Mahoney MW, editors. Friction Stir Welding and Processing. Materials Park, OH (USA): ASM International, 2007, 71-110.

[3]   Y.J. Chao, X. Qi, W. Tang, Heat transfer in friction stir welding: experimental and numerical studies, ASME J. Manuf. Sci. Eng. 125 (2003), 138–145.

[4]   O. Frigaard, O. Grong, and O. T. Midling, A process model for friction stir welding of age hardening aluminium alloys. Metall. Mater. Trans. A. 32(2001), 1189–1200.

[5]   M. J. Russell and H. R. Shercliff H R, 1st Int. Symp. On Friction Stir Welding (Thousand Oaks, California, USA), 1999.

[6]   P. A. Colegrove, H. R. Shercliff, R. Zettler. A model for predicting the heat generation and temperature in friction stir welding from the material properties. Sci. Technol. Weld. Joining 12 (2007), 284–297.

[7]   V. S. Gadakh, and A. Kumar. Heat generation model for taper cylindrical pin profile in friction stir welding. J. Mater.Res. Technol. 2(4) (2013), 370–375.

[8]   P. Ulysse. "Three-dimensional modeling of the friction stir-welding process." Int'l Journal of Machine Tools and Manufacture, 42 (2002), 1549-1557.

[9]   S. Pala, M.P. Phanirajb,∗ Determination of heat partition between tool and workpiece during FSW of SS304 using 3D CFD modeling Journal of Materials Processing Technology 222 (2015) 280–286

[10]   M. B. Đurdanovic, M. M. Mijajlovic, D. S. Milcic, D. S. Stamenkovic, Heat Generation During Friction Stir Welding Process, Tribology in Industry,31 (2009), 1-2, pp. 8-14.

[11]   M. Mijajlović, and D. Milčić Analytical model for estimating the amount of heat generated during friction stir welding: Application on plates made of aluminium alloy. INTECH, Open Science 2024-T351, Chapter 11 (2012) 247–274.

[12]   T. K. Jauhari. Development of Multi-Component Device for Load Measurement and Temperature Profile for Friction Stir Welding Process [M.Sc Thesis]. Penang: UniversitiSains Malaysia; Unpublished. 2012.

[13]   A. Arora, T. Debroy, H. K. D. H. Bhadeshia. Back-of-the-envelope calculations in friction stir welding – velocities, peak temperature, torque, and hardness. Acta Mater 2011; 59:2020–8.

[14]   A. Arora, R. Nandan, A. P. Reynolds, T. DebRoy. Torque, power requirement and stir zone geometry in friction stir welding through modeling and experiments. Scr Mater 60 (2009), 13–16.

[15]   N. S. M. El-Tayeb, K. O. Low, P. V. Brevern. On the surface and tribological characteristics of burnished cylindrical Al-6061. Tribol. Int 42(2009), 320–326

[16]   A. Devaraju, A. Kumar, B. Kotiveerachari. Influence of addition of Grp/Al2O3p with SiCp on wear properties of aluminum alloy 6061-T6 hybrid composites via friction stir processing. Trans Nonferrous Met Soc China 23(2013), 1275–1280

[17]   T. Sheppard and D. Wright. Determination of flow stress. Part 1 constitutive equation for aluminum alloys at elevated temperatures, Met. Technol., 6 (1979), 215–223.

[18]   T. Sheppard and A. Jackson. "Constitutive equations for use in prediction of flow stress during extrusion of aluminium alloys", Materials Science and Technology, 13(3) (1997), 203–209.

[19]   R. K. Uyyuru, S. V. Kallas. Numerical analyses of friction stir welding process. J Mater Eng Perform, 15(2006), 505–518.

[20]   P. A. Colegrove, H. R. Shercliff. CFD Modelling of the friction stir welding of thick Plate 7449 aluminium alloy. Sci. Technol. Weld. Joining 11 (4) (2006), 429–441.

[21]   H. Wang, P. A. Colegrove, J. F. Dos Santos. Numerical investigation of the tool contact condition during friction stir welding of aerospace aluminium alloy. Comput Mater Sci. 71(2013), 101–108.

[22]   H. Su., C. Wu., M. Chen. Analysis of material flow and heat transfer in friction stir welding of aluminium alloys. China Weld (Engl Ed). 22 (2013):6–10.

[23]   H. Schmidt, J. Hattel, and J. Wert. Analytical models for the heat generation in friction stir welding. Modelling Simul. Mater. Sci. Eng. 12(2004): 143–157.

[24]   M. Z. H., Khandkar, J. A. Khan and R. A. Reynolds., Prediction of temperature distribution and thermal history during Friction Stir Welding: Input torque based model, Science & Technology of Welding & Joining., 8(3) (2003), 165-174.

[25]   Hamilton, C., Dymek, S. and Sommer, E. (2008). A Thermal Model for Friction Stir Welding in Aluminum Alloys. Int J Mach Tool Manuf. 2811201130.

[26]   Roy, G. G., Nandan, R. and DebRoy, T (2006). Dimensionless correlations to estimate peak temperature during friction stir welding. SciTechnol Weld Join; 11:606–8.

[27]   R. Nandan, G. Roy, and T. Debroy, Numerical simulation of three-dimensional heat transfer and plastic flow during friction stir welding. Metallurgical and Materials Transactions A, 2006. 37(4) (2006), 1247-1259.